X-ray microtomography for studying localized deformation in fine-grained geomaterials under triaxial compression

Gioacchino Viggiani [a,*], Nicolas Lenoir [a,b], Pierre Bésuelle [a], Marco Di Michiel [c], Stefania Marello [a], Jacques Desrues [a], Mogens Kretzschmer [c]

[a] *Laboratoire 3S, UJF–INPG–CNRS, UMR 5521, BP 53, 38041 Grenoble, France*
[b] *Agence nationale pour la gestion des déchets radioactifs (ANDRA), Châtenay–Malabry, France*
[c] *European Synchrotron Radiation Facility, BP 220, 38043 Grenoble, France*

Abstract

This Note presents a few selected results of an experimental testing program carried out at the ESRF in Grenoble, France. X-ray microtomography (with a spatial resolution of 14 µm) has been used to evaluate the onset and evolution of shear banding in a fine-grained stiff soil under deviatoric loading. It allowed detailed observations of strain localization in a specimen during the test, including the presence of more than one shear zone and a varying degree of dilatancy and/or crack opening. ***To cite this article: G. Viggiani et al., C. R. Mecanique 332 (2004).***
© 2004 Académie des sciences. Published by Elsevier SAS. All rights reserved.

Résumé

Utilisation de la microtomographie rayon X pour l'étude de la localisation des déformations dans les géomatériaux argileux sous sollicitation axisymétrique. Cette Note présente une sélection de résultats obtenus lors d'une campagne d'essais expérimentale menée à l'ESRF de Grenoble. La microtomographie à rayons X a été utilisée afin d'étudier la naissance et l'évolution de bandes de cisaillement lors d'un chargement déviatorique dans un sol fin et raide. La reconstitution tomographique (avec une résolution spatiale de 14 µm) permet une observation détaillée du phénomène, montrant plusieurs zones de cisaillement et une évolution du niveau de dilatance et/ou d'ouverture de fissures. ***Pour citer cet article : G. Viggiani et al., C. R. Mecanique 332 (2004).***
© 2004 Académie des sciences. Published by Elsevier SAS. All rights reserved.

---

* Corresponding author.
E-mail address: cino.viggiani@hmg.inpg.fr (G. Viggiani).

Version française abrégée

Le phénomène de localisation de la déformation, pouvant être décrit comme une concentration de la déformation à l'intérieur d'une zone étroite, est très fréquemment observé dans les géomatériaux [1]. Les études expérimentales destinées à caractériser la transition d'un mode diffus de déformation vers un mode localisé nécessitent une mesure de champ [3]. De ce fait, la possibilité qu'offre la tomographie rayons X d'une reconstruction tridimensionnelle est exploitée depuis plusieurs années. Toutefois, il est très difficile à la fois de charger un échantillon pour induire une localisation de la déformation, de contrôler la pression du fluide remplissant sa porosité et d'effectuer des mesures tomographiques. De plus, les matériaux argileux comme celui étudié ici, présentent des épaisseurs de bande très fines qui nécessitent une très bonne résolution spatiale de la mesure. L'utilisation du rayonnement synchrotron dont le faisceau est très puissant permet de satisfaire ces exigences, à la fois une haute résolution spatiale et une rapidité de mesure. L'article présente un programme d'essai mené à l'ESRF de Grenoble (ligne ID15) sur une marne et pour lequel une cellule de pression transparente aux RX a été spécifiquement développée.

Le dispositif de la ligne ID15 permet de reconstruire le champ d'absorption aux RX sur des coupes perpendiculaires à l'axe de l'échantillon cylindrique (diamètre 20 mm et hauteur 40 mm). La taille d'un voxel (unité spatiale de mesure) est de $14 \times 14 \times 14 \ \mu m^3$. La mesure d'une tranche comportant 128 coupes peut être exécutée en à peu près 3,5 minutes. La cellule d'essai permet quant à elle, en mettant un fluide sous pression, d'appliquer une pression radiale de confinement sur le matériau via une membrane souple et étanche, de même qu'une pression axiale de chargement via un piston pour induire du cisaillement dans l'échantillon, et aussi une pression de pore. Le matériau (marne de Beaucaire) est argileux et comporte pour 60 %, des particules de taille entre 2 et 60 µm, et 30 % des particules de taille inférieure à 2 µm. Cinq essais ont été menés à différentes pressions de confinement, soit en conditions drainées (pression interstitielle constante), soit en conditions non drainées (masse du fluide interstitiel constant).

Un seul de ces essais (réalisé en conditions drainées) est présenté ici en détail. La courbe déviateur de contrainte en fonction de la déformation axiale (Fig. 2) montre une croissance, suivie d'un pic, d'un radoucissement et d'un plateau. L'échantillon est contractant dans la phase initiale du chargement puis devient dilatant avant la phase de radoucissement. Deux séries de coupes tomographiques sont montrées (Fig. 3), correspondant à deux hauteurs sur l'axe de l'échantillon. Cinq mesures tomographiques ont été réalisées à différentes étapes du chargement. La localisation de la déformation devient visible après la phase de radoucissement (étape c de la Fig. 2 et troisième colonne de la Fig. 3). Les structures de localisation sont composées à la fois de petites bandes de localisation dilatantes et de fissures ouvertes, les unes prenant le relais des autres. D'une manière plus globale, on constate que l'évolution de la structure de localisation est complexe, composée de plus d'une zone de cisaillement, que celles-ci ne sont pas planes et qu'elles présentent un degré de dilatance ou d'ouverture variant à la fois dans le temps et dans l'espace. On peut dans certains cas observer au cours du chargement la transition entre une bande de dilatance et une fissure ouverte [12]. Les structures de localisation ont une épaisseur de l'ordre de 40 à 50 µm. Elles sont extrêmement concentrées en ce sens qu'aucun gradient de densité n'a pu être observé autour des bandes (compte tenu de la résolution spatiale de la mesure).

1. Background

Strain localization, the concentration of deformation into narrow zones of intense shearing, is a phenomenon commonly observed in virtually all geomaterials, including rocks, soils and concrete. The body of literature on the modeling of localization in geomaterials has been growing rapidly during the last few decades, see for example [1]. Various experimental studies have also been carried out (e.g., [2,3]). A wide range of experimental techniques have been applied over the years, which include optical and electronic microscopy, radiographic analysis, ultrasonic and acoustic techniques, multiple local stress and strain measurements, stereophotogrammetry and image analysis. The challenge here, and the possible reason why so many different techniques have been used is that one wants

to measure deformations in a region the size of which, upon strain localization, reduces abruptly and dramatically, say from the scale of the specimen to the shear band scale. Measuring deformations throughout a test, that is: prior to, at, and after the onset of strain localization is then a formidable task, which can only be accomplished by using *field* measurements. In fact, when strains are (highly) localized, stress and strain variables cannot be derived from boundary measurements of loads and displacements.

The recently developed nondestructive 3D imaging techniques, such as X-ray tomography (e.g., [4]), offer new experimental possibilities for studying shear banding and failure, in that they allow for direct observation of the internal structure of a specimen while it deforms under applied load. However, there is one main difficulty with using such a tool in geomechanics. In fact, the multiphase nature of soils (a solid skeleton and a pore fluid, in the simplest case of complete saturation) imposes special requirements for testing. In particular, total stresses and pore pressures must be controlled and measured separately so effective stresses, which govern soil behavior, can be determined. Drainage of the pore fluid into, or out of, the specimen must be controlled so that tests may be either drained (i.e., constant pore pressure) or undrained (i.e., constant volume). It appears that these requirements make it quite difficult to properly run a test within a typical X-ray tomography set up, especially if one intends to perform in situ tomography, i.e., to load the specimen and to scan it in the same setting and at the same time. To our knowledge, there is only one study where this was fully achieved [5], whereas in other previous applications of X-ray tomography for studying shear banding in soils and rocks either the compression test and the scanning were not conducted simultaneously (e.g., [6,7]), or no control of effective stress was implemented (e.g., [8,9]). A state-of-the-art on the application of X-ray tomography to rock has been presented recently [10], to which the interested reader is referred.

2. X-ray microtomography

X-ray absorption tomography involves recording of radiographies of a specimen at different angular positions and reconstructing a 3D image from the spatial distribution of the linear attenuation coefficient. High resolution X-ray tomography (*microtomography*) methods have been developed over the last two decades, their typical set up including a simple projection geometry with a high resolution imaging detector and a highly collimated beam, such as a *synchrotron* radiation source. The system used in this research allows performing microtomography of a specimen under load (in situ), using a specifically built load frame that could be placed in the X-ray beam. The experiments were carried out at the high energy beam line ID15 at the European Synchrotron Radiation Facility (ESRF) in Grenoble, France. The setup is schematically shown in Fig. 1(a). The triaxial loading system sits on a translation and rotation stage so that it can be viewed, at different elevations, from the many different angles required for tomographic data collection. The X-ray white beam is generated by an 11 poles wiggler and filtered to remove low energy photons in order to avoid beam hardening artifacts. A fast shutter is used to get short exposure times. The X-ray energy used here ranges from about 50 to 70 keV, allowing the X-rays to go through the two
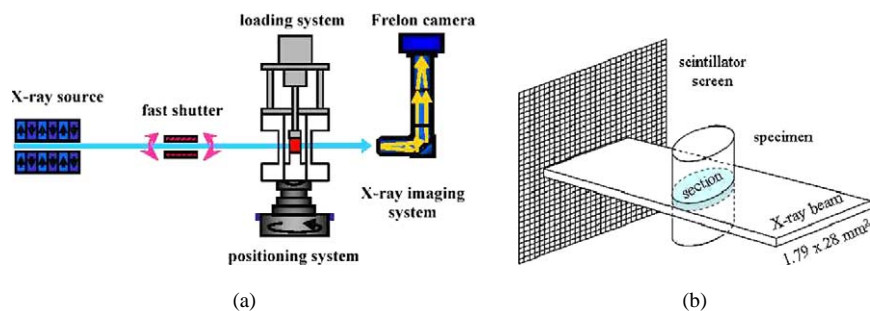

Fig. 1. (a) Experimental set up for microtomography; (b) X-ray beam through the specimen to the scintillator.

5 mm thick Plexiglas cell walls, the confining fluid, and the 20 mm diameter clay specimen. The scintillator is a Gadox fluorescent screen which transforms the X-rays into visible light. A 2048×2048 CCD Frelon camera captures the raw digital images from the fluorescent screen. A $1\times$ objective was used, which produced images with a 28 mm wide field of view. The thickness of a tomographic section of the specimen, which corresponds to the width of the X-ray beam, is 1.79 mm. Each radiograph generates a 1.79×28 mm^2 image which corresponds to 128×2048 pixels on the CCD camera (see Fig. 1(b)). The complete scan of a section was obtained by taking 1200 radiographies at different equally spaced angles covering a range of 180° with an exposure time of 0.08 s for each one. Each section of the specimen could be scanned in approximately 3.5 min, this value being dictated by the shutter opening/closing time, exposure time, and the read out time. After mathematical reconstruction, one obtains 128 2D images ('slices', hereafter) for each section of the specimen. The slices are orthogonal to the axis of rotation of the specimen during the scans. The voxel size is $14 \times 14 \times 14$ µm^3, i.e., a relatively high spatial resolution.

It is worth noting that to achieve both high resolution (for a relatively large scanned body) and fast scanning, a high photon flux is needed. This cannot be obtained with conventional Computed Tomography (CT) systems, such as those used in medical and industrial applications. With the only exception of [10], all the experimental studies mentioned in Section 1 were performed with conventional CT, whereas synchrotron radiation microtomography has been used herein for the first time to evaluate the onset and evolution of (extremely) localized deformation in a saturated fine-grained stiff soil under deviatoric loading.

3. Material tested, experimental apparatus and procedure

The material tested for this study (*Beaucaire Marl*) is a sedimentary soil which has been extensively studied at the Laboratoire 3S in Grenoble over the last fifteen years. It comes from a natural deposit located at Beaucaire (France), which was deposited in a shallow marine environment during the Pliocene age. The material is a clayey silt, with about 60% in weight of the solid particles having an equivalent diameter in the range 2–60 µm and 30% less than 2 µm. The calcium carbonate content can be as high as 34%, and the specific gravity of the solids, G_s, is equal to 2.75. Microscopic observation did not reveal any evidence of pre-existing micro-cracks. The natural material is heavily overconsolidated and quite stiff, its natural water content ranging from 16 to 21%, which should be compared to a liquid limit and a plasticity index in the range 38–41% and 21–25%, respectively. The vertical yield stress from 1D compression tests is about 2 MPa, and its uniaxial compressive strength averages 0.9 MPa. The 'intact' specimens for the experimental program described in this paper were obtained using a diamond wire saw, which minimizes material disturbance during preparation.

The experimental apparatus includes a small triaxial cell and a loading device designed specifically for this program. The triaxial apparatus is practically the same as a conventional triaxial testing system, except for its much smaller size and the shape of the confining cell, which was designed to be transparent to the X-rays. The soil specimen is a cylinder with height twice the diameter (40 and 20 mm, respectively). The top and bottom rigid platens are enlarged and lubricated to minimize friction at the ends of the specimen. The specimen is enclosed in a thin latex sleeve sealed to the top and bottom platens; the sleeve acts both as a flexible membrane and as a seal to separate pore fluid pressures, u, and total stresses, σ. The sealed specimen is placed in a de-aired water-filled cell, which can sustain up to 1 MPa. The bottom platen houses a 6 mm diameter, high air-entry-value-pressure porous stone connected to the drainage line passing through the base of the cell to pore pressure and volume change measuring equipment. A frictionless ram passes through the top of the cell and allows applying a stress deviator $q = (\sigma_a - \sigma_r)$, σ_a and σ_r being the axial and radial total stress, respectively. The specimen is subjected to a mean total stress $p = (\sigma_a + 2\sigma_r)/3$, and mean effective stress $p' = (p - u)$. The axial strain, ϵ_a, is obtained by measuring the movement of the ram using a LVDT. The axial load and hence the deviator stress is applied in a displacement-controlled manner using a motor-driven screw actuator. The loading system was designed specifically for this program (in cooperation with *CSP – Composants et Systèmes de Précision*) and can be placed in the

X-ray beam line without interfering with the tomographic scans. It is quite compact and light (less than 30 kg), which is important since it sits directly on the translation and rotation stage during the experiment. The system has a maximum loading capacity of 7.5 kN and allows to move the ram at a constant rate in the range of 1 to 100 µm/min. Contrary to a conventional system, the tensile reaction force in this case is carried by the cell walls and not a loading frame. This provides a clear path to the specimen for the X-ray beam, free of any obstacle (apart from the cell walls).

For each test, an isotropic consolidation phase (with zero deviator stress and mean total stress, p_0, equal to the cell pressure) preceded the actual triaxial compression (deviatoric) phase. As it is customary in soil testing, a back pressure $u_0 < p_0$ was applied to the pore water, its purpose being to saturate the specimen (and the drainage lines) by dissolving any air or gas present in the pore water. Provided that the results are expressed in terms of Terzaghi effective stress, the magnitude of the back pressure (approximately equal to 200 kPa in these experiments) has no influence on the test. Opening the drainage lines allowed consolidation (or swelling, depending on the final value of mean effective stress), i.e. the dissipation (in time) of excess pore pressure in the specimen. Each specimen was in an isotropic state of effective stress, p'_0, at the end of consolidation, which took from 6 to 12 hours on average, essentially depending on the initial degree of saturation of the drainage lines (the permeability of Beaucaire Marl is in the order of 10^{-9} m/s, which is relatively high for a stiff fine-grained soil). Volume changes were recorded during consolidation. In addition, three complete tomographic sections of the specimen were taken before and at the end of the consolidation phase of each experiment. The subsequent phase of deviatoric loading was performed under displacement control, by advancing the loading ram at a rate of 3 µm/min, which corresponds to a nominal axial strain rate of 0.45 %/hour for a 40 mm specimen height. The ram displacement was stopped at different levels of axial strain, i.e., when a tomographic scan of the specimen was required. The specimen was scanned while the axial strain was held constant, which unavoidably causes some amount of axial load relaxation during scanning. However, the scanning operations were fast enough (approximately 40 minutes for three sections and 120 minutes for eleven adjacent sections) for this relaxation to be relatively small. A total of five tests were performed, under either drained or undrained conditions. All specimens had a degree of saturation close to 100% before testing.

4. Selected results

Results from only one experiment (drained test XD02) are presented herein as an example of the information that microtomography was able to provide on strain localization in Beaucaire Marl. Fig. 2 shows the relevant curves of deviator stress q and volumetric strain ϵ_v as a function of axial strain ϵ_a as recorded during the test. Deviator stress is computed by dividing the force in the loading ram by the current cross-sectional area of the specimen. Axial strain is computed as $\epsilon_a = -\ln(H/H_0)$, where H_0 and H are the initial and current height of the specimen, respectively. Similarly, $\epsilon_v = -\ln(V/V_0)$, where V_0 and V are the initial and current volume of the specimen, respectively. All stresses and strains are positive in compression. In test XD02, the deviator stress first
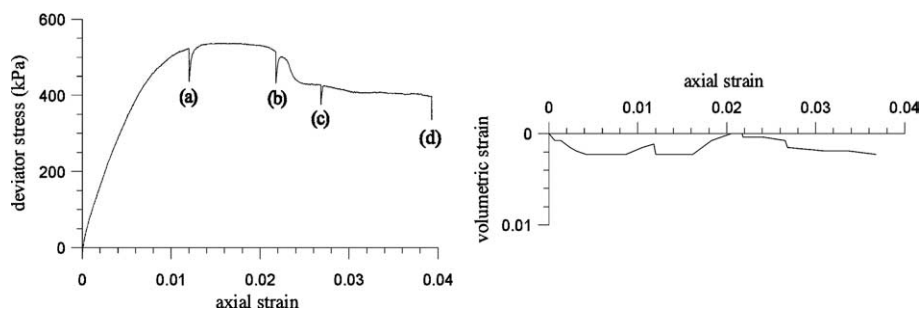

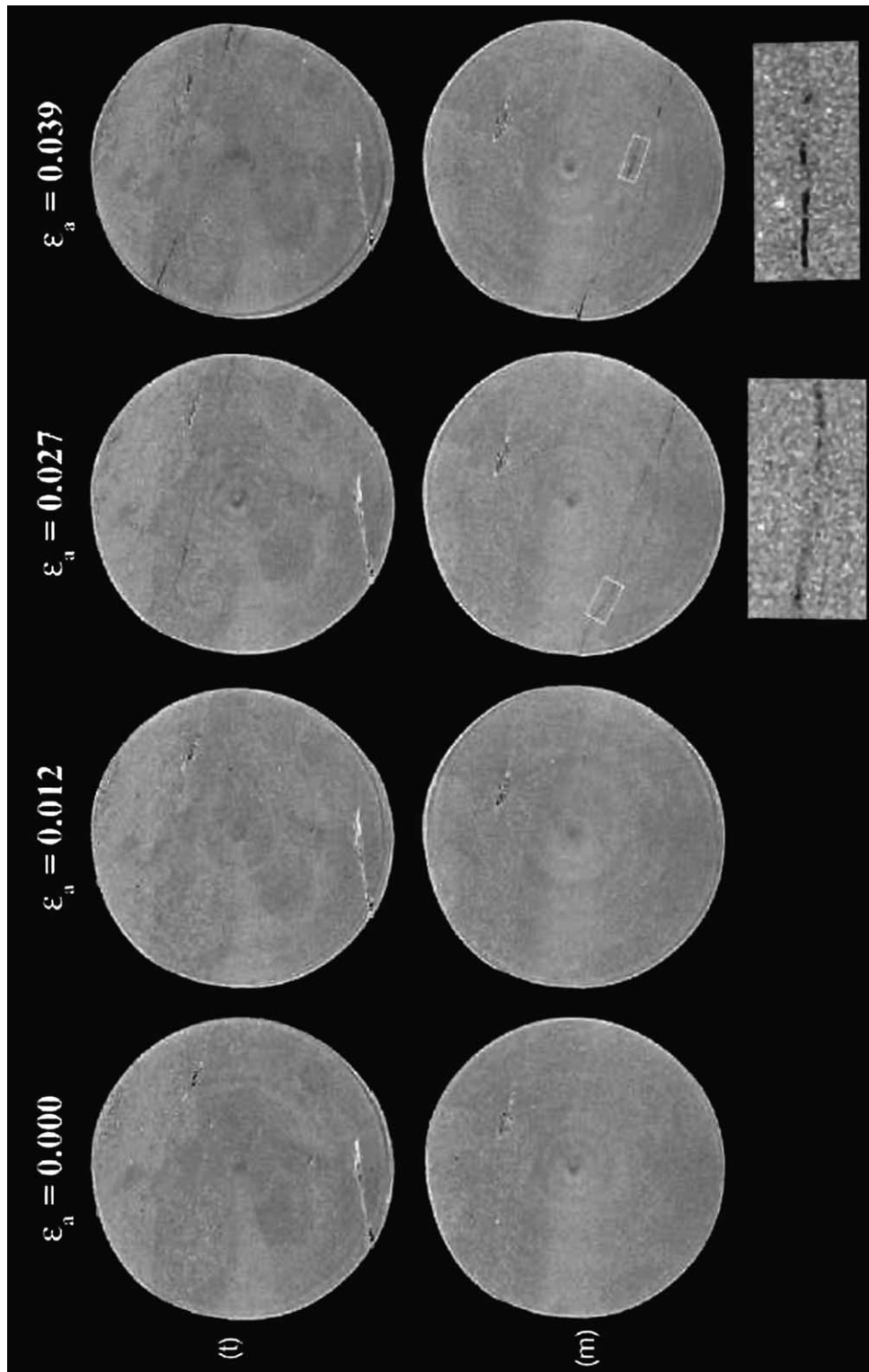Fig. 2. Stress strain response from drained test XD02 on Beaucaire Marl.

Fig. 3. 2D reconstructed cross-sectional slices of specimen XD02: top and bottom row correspond to top (t) and middle (m) sections, respectively.

increases, then reaches a plateau and finally decreases at an axial strain of approximately 0.021. Afterwards, the deviator stress essentially levels off. The global volumetric response is initially contractive, then dilative before an essentially zero slope is finally attained as the deviator stress levels off. A short interval of more pronounced dilative behavior occurs just before the drop of deviator stress. The four small unloading–reloading branches on the q versus ϵ_a curve in Fig. 2 indicate the points of the test when the ram was stopped and several cross sections of the specimen were scanned.

A single shear band formed in the specimen during the test, which could be clearly observed by the eye at the end of the test. This zone of localized deformation seems fairly planar throughout the specimen. A series of cross-sectional tomographic slices of the specimen are shown in Fig. 3, at two different elevations (top, t, and middle, m) from the base of the specimen. The slices were taken just before deviatoric loading ($\epsilon_a = 0$) and at four states during the test ((a) to (d)). Note that to take into account the specimen shortening during a test, the elevation of a given tomographic slice decreases from one scan to the next, such that the material section considered is always the same. While no localization was observed in scans (a) and (b), scan (c) at $\epsilon_a = 0.027$ reveals some narrow regions of localized deformation both in the middle and top sections of the specimen. The zoom at the bottom of the third column in Fig. 3 (where the image size has been magnified by 6) shows that the material is dilating (darker indicates lower mass density) in the bands of localized deformation. The thickness of the bands is always at least three times the system resolution, i.e. in the order of 40 to 50 μm. Moreover, the bands include a few segments which can be interpreted as open cracks (black indicates no solid matter), a few pixels wide. At the end of the test (scan (d) at $\epsilon_a = 0.039$), the regions of localization look like non-continuous cracks, connected by very thin shear bands (zoomed image at the bottom of fourth column, magnified by 6). Overall, this observed pattern of localization evolution is relatively complex. Some clear features to point out include the presence of more than just one shear zone, a curved shape, and a varying degree (in time and space) of dilatancy and/or crack opening. What the images do not necessarily bring out is a clear picture of why localization took place precisely where it did. In particular, there does not appear to be any evidence of zones of strain localization emerging from inclusions or other 'defects' in the natural material (such as, for example, the white streak visible in the upper slices in Fig. 3). Rather, strain localization appears in material that visually seems to be quite sound.

Besides illustrating how strain localization progressed in the specimen, microtomography also provided a direct evaluation of the effects of specimen preparation. The images in Fig. 3 indicate that wire saw cutting 'damages' the specimen in that it increases the soil density all around. However, this is only a skin effect (the affected thickness is less than 0.3 mm, which implies that, despite their relatively small size, the tested specimens can be fairly considered as 'undisturbed').

Finally, it is worth recalling that so-called hardening artifacts can be excluded, because of the X-ray beam filtering which removes low energy photons. However, the tomographic images in Fig. 3 still show some unavoidable, minor artifacts (generally referred to as 'ring artifacts') which appear as black circle arcs at the edges of the specimen.

5. Conclusions

This experimental program used synchrotron radiation microtomography to evaluate the onset and evolution of localized deformation in a saturated fine-grained stiff soil under deviatoric loading. A loading system was specifically designed to be placed in the X-ray beam and to meet in the mean time all the requirements for testing a saturated soil specimen. Recently used for studying damage evolution in mortars [11], in situ synchrotron radiation microtomography is used here for the first time for saturated geomaterials.

In total, five tests were performed on natural specimens of Beaucaire Marl, although results from just one have been discussed in full. A few results from the other tests have been presented elsewhere [12]. Based on the entire set of X-ray microtomography observations, it can be concluded that the pattern of localization in Beaucaire Marl is quite complex. Both dilating shear bands (which are visible in tomography as bands of localized dilatancy) and

cracks were observed to form and to interact in the course of deformation. In some cases, dilating shear bands evolved to cracks in the course of deformation. The regions of localization are in any case extremely thin (in the order of 40 to 50 microns), which sometime makes it difficult to discriminate between a dilating shear band and a crack propagating in shear.

The most striking observation that can be made from the X-ray scans obtained in this study is that there is no gradual change of soil density from the zone of localization to the zones of the specimen far from the crack. In other words, no density gradient can be observed (within the resolution of the method) on the two sides of the zone of localization. This indicates that, whatever its nature (crack or dilating shear band), localization in Beaucaire Marl is absolutely sharp in space. A number of thin sections from the tested specimens are currently in preparation for SEM micro structural observation, which will shed further light on this particular feature. The tomographic images show that, at a given stage of the deformation process, the region of localization itself can be quite non-uniform, and that the dilatancy inside the band (or the aperture of the crack, in case of a strong discontinuity) is typically higher close to the specimen lateral boundaries than in the core of the specimen.

While microtomography allowed very detailed observations of strain localization, the results presented herein are only a first step of the research. The next, essential steps will include the reconstruction of three dimensional X-ray attenuation distributions from a series of cross-sectional slice images, and the quantitative analysis of density evolution in the specimen throughout a test. While getting a 3D reconstruction is relatively straightforward, the quantitative analysis of density is not trivial for a natural fine-grained soil, because X-ray absorption depends on both mineralogy and porosity.

References

[1] I. Vardoulakis, J. Sulem, Bifurcation Analysis in Geomechanics, Blackie Academic & Professional, Glasgow, 1995.
[2] A.S. Saada, G. Bianchini, L. Liang, Cracks, bifurcation and shear bands propagation in saturated clay, Géotechnique 44 (1994) 35–64.
[3] J. Desrues, G. Viggiani, Strain localization in sand: an overview of the experimental results obtained in Grenoble using stereophotogrammetry, Int. J. Num. Anal. Meth. Geomech. 28 (4) (2004) 279–321.
[4] J. Baruchel, J.Y. Buffière, E. Maire, P. Merle, G. Peix, X-ray Tomography in Materials Science, Hermes, Paris, 2000.
[5] J. Otani, T. Mukunoki, Y. Obara, Characterization of failure in sand under triaxial compression using an industrial X-ray scanner, Int. J. Phys. Model. Geotechnics 1 (2002) 15–22.
[6] J. Desrues, R. Chambon, M. Mokni, F. Mazerolle, Void ratio evolution inside shear bands in triaxial sand specimens studied by computed tomography, Géotechnique 46 (1996) 529–546.
[7] K.A. Alshibli, S. Sture, N.C. Costes, M.L. Franck, M.R. Lankton, S.N. Batiste, R.A. Swanson, Assessment of localized deformation in sand using X-ray computed tomography, Geotechnical Testing J. ASTM 23 (2000) 274–299.
[8] H.J. Vinegard, J.A. de Waal, S.L. Wellington, CT studies of brittle failure in Castlegate sandstone, Int. J. Rock Mech. Min. 28 (1991) 441–448.
[9] H. Kawakata, A. Cho, T. Kiyama, T. Yanagidani, K. Kusunose, H. Shimada, Three-dimensional observations of faulting process in Westerly granite under uniaxial and triaxial conditions by X-ray CT scan, Tectonophysics 313 (1999) 293–305.
[10] A. Vervoort, M. Wevers, R. Swennen, S. Roels, M. Van Geet, E. Sellers, Recent advances of X-ray CT and its application for rock material, in: J. Otani, Y. Obara (Eds.), X-ray CT for Geomaterials (GeoX2003), Balkema, 2004, pp. 79–91.
[11] E.N. Landis, E.N. Nagy, D.T. Keane, Microstructure and fracture in three dimensions, Eng. Fract. Mech. 70 (2003) 911–925.
[12] N. Lenoir, S. Marello, G. Viggiani, P. Bésuelle, J. Desrues, M. Di Michiel, X-ray micro tomography characterization of strain localization upon deviatoric loading of saturated fine-grained stiff soils, in: J. Otani, Y. Obara (Eds.), X-ray CT for Geomaterials (GeoX2003), Balkema, 2004, pp. 147–155.